UC Davis

UC Davis Previously Published Works

Title

Trans-ocular Electric Current In Vivo Enhances AAV-Mediated Retinal Gene Transduction after Intravitreal Vector Administration

Permalink

https://escholarship.org/uc/item/0c41p03d

Authors

Song, Hongman
Bush, Ronald A
Zeng, Yong
et al.

Publication Date

2019-06-01

DOI

10.1016/j.omtm.2018.12.006

Peer reviewed

eScholarship.org Powered by the California Digital Library
University of California

Molecular Therapy
Methods & Clinical Development
Original Article

Trans-ocular Electric Current *In Vivo* Enhances AAV-Mediated Retinal Gene Transduction after Intravitreal Vector Administration

Hongman Song,[1] Ronald A. Bush,[1] Yong Zeng,[1] Haohua Qian,[2] Zhijian Wu,[2] and Paul A. Sieving[1,2]

[1]Section for Translational Research on Retinal and Macular Degeneration, National Institute on Deafness and Other Communication Disorders, Bethesda, MD 20892, USA; [2]National Eye Institute, NIH, Bethesda, MD 20892, USA

Adeno-associated virus (AAV) vector-mediated gene delivery is a promising approach for therapy, but implementation in the eye currently is hampered by the need for delivering the vector underneath the retina, using surgical application into the subretinal space. This limits the extent of the retina that is treated and may cause surgical injury. Vector delivery into the vitreous cavity would be preferable because it is surgically less invasive and would reach more of the retina. Unfortunately, most conventional, non-modified AAV vector serotypes penetrate the retina poorly from the vitreous; this limits efficient transduction and expression by target cells (retinal pigment epithelium and photoreceptors). We developed a method of applying a small and safe electric current across the intact eye *in vivo* for a brief period following intravitreal vector administration. This significantly improved AAV-mediated transduction of retinal cells in wild-type mice following intravitreal delivery, with gene expression in retinal pigment epithelium and photoreceptor cells. The low-level current had no adverse effects on retinal structure and function. This method should be generally applicable for other AAV serotypes and may have broad application in both basic research and clinical studies.

INTRODUCTION

Recombinant adeno-associated viral (AAV) vectors show promise for ocular gene therapy, with positive safety and efficacy results demonstrated in preclinical studies and clinical trials.[1–8] Successful clinical application of AAV-based gene therapies requires efficient transduction and expression by target cells. Because many inherited retinal degenerations involve genes expressed in photoreceptors and retinal pigment epithelium (RPE),[9,10] these are important cells for therapeutic gene expression.

The route of gene administration affects the efficacy of retinal AAV-mediated gene therapy. Commonly used AAV serotypes 1, 2, 5, 8, and 9 efficiently transduce the RPE and/or photoreceptors in the wild-type (WT) adult rodent retina only when given by subretinal injection.[11–18] Unfortunately, this limits vector distribution primarily to the region surrounding the site of subretinal administration.[19,20] This approach may also cause injury particularly for degenerative and surgically vulnerable retinal conditions.[2,7,17,21,22] Intravitreal injection is more desirable as a less invasive way to deliver AAV vectors to the retina.[23] Following intravitreal injection, AAV vectors diffuse through the vitreous humor and distribution theoretically reaches the entire retina. However, the extensive laminated structure of the vertebrate retina further limits AAV vectors from reaching cells in outer retina after vitreous application, and these RPE and photoreceptor cells often show limited transduction.[11,12,15–17,24,25] Approaches to overcome such tissue barriers (e.g., diffusion and membranes) include mild enzymatic digestion of the inner limiting membrane (ILM),[26,27] vitrectomy,[28] and surgical ILM peeling.[29] This sometimes yields enhanced AAV transduction, but a more efficient and convenient method would be useful.

We explored the use of low electric current stimulation applied across the eye *in vivo* to enhance retinal delivery of therapeutic AAV vector constructs administered into the vitreous. Several points are worth noting in support of this strategy: AAV is an icosahedral non-enveloped single-stranded (ss) DNA virus that is relatively thermostable and resistant to mild proteolytic digestion and nonionic detergents. It has an overall net negative charge in a neutral environment.[30] Mobility and migration of norovirus, an ssRNA virus having a structure similar to AAV, is enhanced across a membrane barrier by applying an electric field.[31] Trans-ocular electric current (iontophoresis) is known to facilitate tissue and cellular penetration of oligonucleotide and plasmid DNA,[32–38] and low-level electrical stimulation (ES) *in vivo* has been shown to be safe and potentially even neuroprotective to animal and human eyes with retinal degeneration.[39–41]

In this study, we developed and tested a novel, non-invasive approach of electric-current vector mobility (ECVM) with intravitreal vector injection and showed that this strategy significantly improves the transduction efficiency of AAV8 vectors in WT mouse retina. Although only AAV8 was tested in the current study, this approach

Received 30 August 2018; accepted 14 December 2018;
https://doi.org/10.1016/j.omtm.2018.12.006.

Correspondence: Paul A. Sieving, National Eye Institute, NIH, 31 Center Drive, Room 6A03, Bethesda, MD 20892, USA.
E-mail: paulsieving@nei.nih.gov

This is an open access article under the CC BY-NC-ND license (http://creativecommons.org/licenses/by-nc-nd/4.0/).

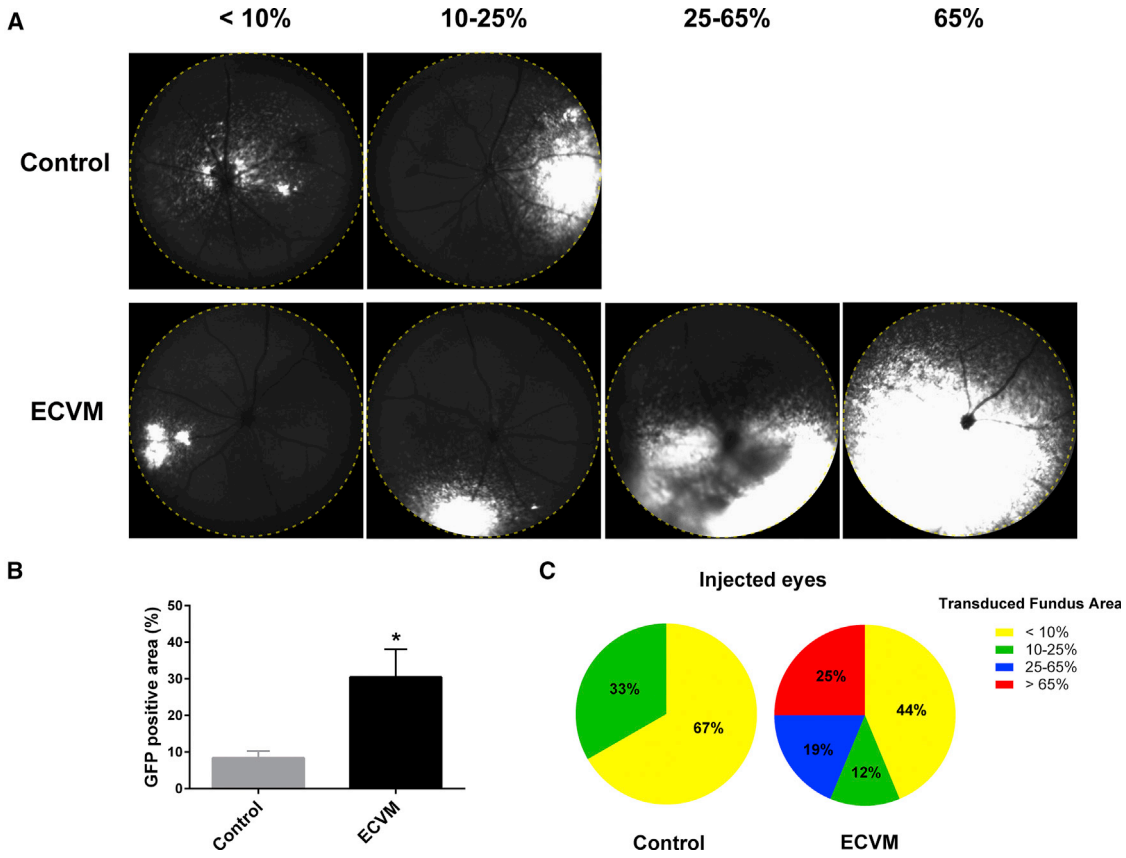

Figure 1. The Approach of Electro-Current Vector Mobility Significantly Enhances AAV8-Mediated Gene Transduction in Wild-Type Retinas following Intravitreal Delivery (1×10^9 vg/eye)

WT mouse eyes were treated with ECVM (continuous direct current 10 μA/20 min) immediately after intravitreal injection of AAV8-CMV-EGFP. Vector-injected WT eyes without applying ECVM served as controls. Fundus images were taken at 6 weeks post-injection (PI). (A) Representative fundus images of injected-ECVM treated eyes (ECVM) and injected eyes without applying current (control) are shown from samples with different GFP expression (<10%, 10%–25%, 25%–65%, >65%) in terms of fundus area transduced. Dashed circle outlines the central retina. (B) GFP-positive areas of fundus images were quantified and represented as an average percentage of the fundus area showing GFP expression (mean ± SEM) for control (n = 21) and ECVM (n = 16) groups, respectively. *$p < 0.05$, Mann Whitney test. (C) Pie graphs show the probability of injected eyes having a GFP-positive area coverage more than 65%, between 25% and 65%, between 10% and 25%, and less than 10%.

is expected to work with other AAV serotypes and may have broad applications in both basic research and clinical studies.

RESULTS

Our preliminary studies indicated that 10 μA direct current for 20 min did not adversely affect ocular structure or function (see Figures S1 and S2, described in the Materials and Methods). We did not observe whitening of the cornea or the lens for 10 μA current applied for 20 min. Compared with baseline, retinal electroretinography (ERG) function of rod and cone responses showed no change to amplitude or timing after 10 μA direct current (DC), and the intensity-response curves of a- and b-wave responses were unchanged. We then evaluated whether this would enhance the retinal transduction efficiency of AAV8-CMV (cytomegalovirus)-GFP when applied immediately after 1×10^9 vector genomes (vg) were injected into the vitreous of the mouse eye. Control eyes were injected with the GFP vector, but no current was applied. GFP expression was evaluated at 6 weeks post-injection (PI) by *in vivo* fundus imaging. The extent of the retinal area showing GFP expression (expressed in percent; Figure 1A) was used to indicate efficiency of AAV8 vector transduction.

The mean GFP-expressed retinal area was significantly larger in eyes that were treated by the approach of ECVM (30.5%) than for the control group (8.4%; $p = 0.038$, Mann-Whitney test; Figure 1B). Most control eyes (14 of 21, 67%) showed GFP expression across less than 10% of the central retina, and no control eyes showed more than 25% of the central retinal area transduced (Figures 1A and 1C). By comparison, 7 of 16 (44%) injected eyes that received trans-ocular current showed more than 45% of the central retinal area transduced, and 4 of 16 (25%) eyes had GFP expression covering more than 65% of the central retina. These results indicate that ECVM significantly promotes the transduction efficiency of AAV8-CMV-GFP in WT mouse retina following intravitreal injection.

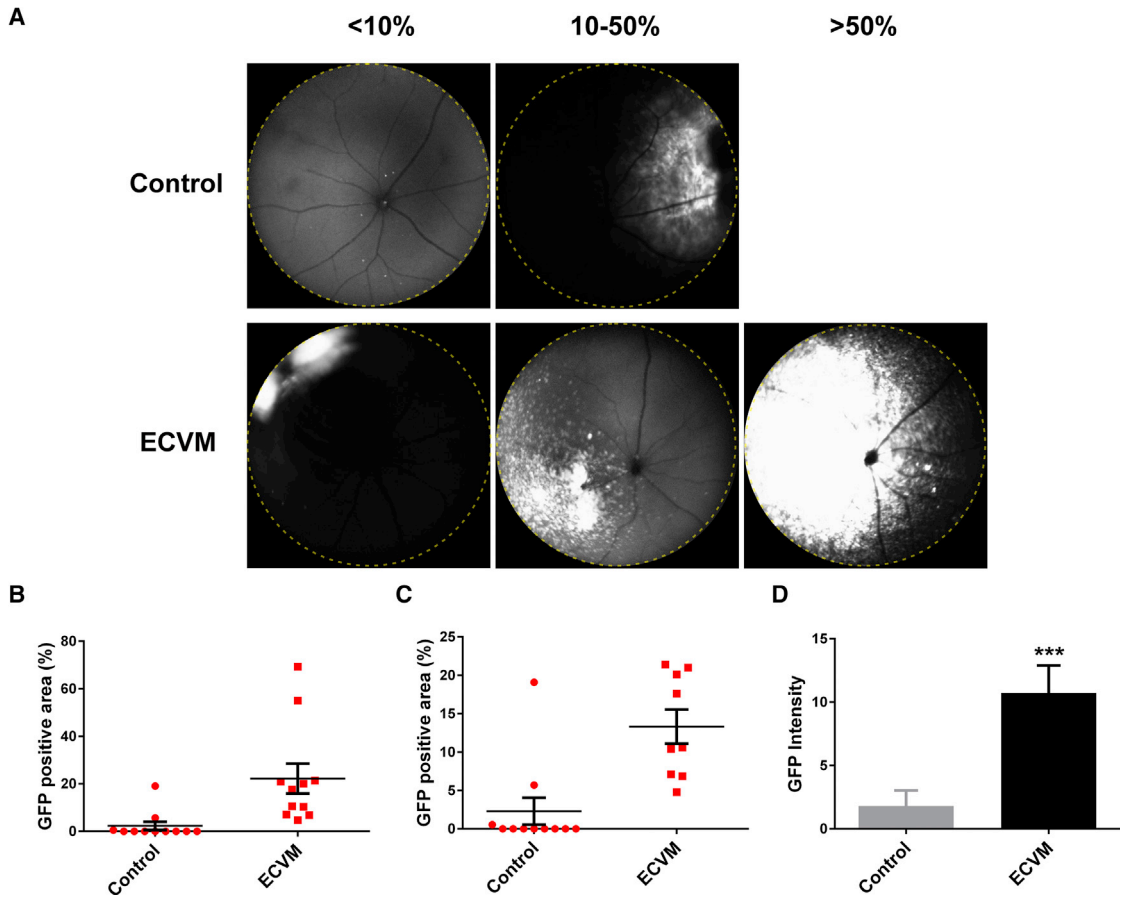

Figure 2. ECVM Increases Transduction Efficacy of AAV Vectors in WT Retinas from the Vitreous at a Reduced Vector Dose (5×10^8 vg/eye)

WT mouse eyes were treated with ECVM (continuous direct current, 10 μA/20 min) immediately after intravitreal delivery of AAV8-CMV-EGFP. Vector-injected WT eyes without ECVM application served as controls. Fundus images were taken at 4.5 weeks post-injection (PI). (A) Representative fundus images of injected eyes with (ECVM) and without electric current (control) were shown from samples with different GFP expression (<10%, 10%–50%, >50%) in terms of fundus area transduced. Dashed circle outlines the central retina. (B) GFP-positive area of the fundus image from each sample was quantified and represented as a percentage of the fundus area showing GFP expression ($p < 0.0001$, Mann Whitney test; $n = 11$ for each group). (C) The difference between two groups was highly significant with two samples showing largest retinal area transduced (outliers) removed from the ECVM group ($p = 0.0003$, Mann Whitney test; $n = 9$ for ECVM group and $n = 11$ for control group). (D) GFP immunofluorescence of representative retinal sections was quantified and plotted as GFP intensity (pixel/area, mean ± SEM) for control and ECVM groups, respectively. ***$p = 0.0007$, Mann Whitney test.

We also evaluated the outcome with a smaller dose of 5×10^8 vg/eye and performed the analysis earlier after intravitreal injection, at 4.5 weeks (Figure 2). This increased the disparity between ECVM-treated and non-treated eyes. Of eyes without ECVM application, 82% (9 of 11) showed no GFP expression across the central retina (Figures 1, 2A, and 2B). By comparison, almost half of eyes receiving ECVM had GFP expression across >20% of the central retina, and 2 of 11 treated eyes had >50% of the central retina transduced. The mean retinal area of GFP expression was significantly greater in the ECVM-treated eyes (22%) compared with injected controls that did not receive current (2.3%; $p < 0.0001$, Mann Whitney test; Figure 2B). We noted that two eyes showed more expression than the remaining nine eyes receiving ECVM treatment. Out of an abundance of caution, we re-ran the analysis after first removing these two samples, assuming they possibly had an anomalously large retinal area transduced. The difference of ECVM-treated ($n = 9$) versus control ($n = 11$) eyes was still highly significant ($p = 0.0003$, Mann Whitney test; Figure 2C).

We then collected the eyes in this lower dose group of 5×10^8 vg/eye and compared GFP expression intensity by immunofluorescence on retinal histologic cryosections at 5 weeks after injection. Injected eyes receiving ECVM application showed about a 6-fold (5.9 ± 1.2) higher intensity compared with the control eyes ($p = 0.0007$, Mann-Whitney test; Figure 2D). These further support the finding that trans-ocular ECVM increased the retinal transduction efficacy of AAV vectors following intravitreal administration.

We also evaluated the distribution of retinal cells transduced by the AAV8-EGFP in ECVM-treated eyes. GFP was observed in all retinal

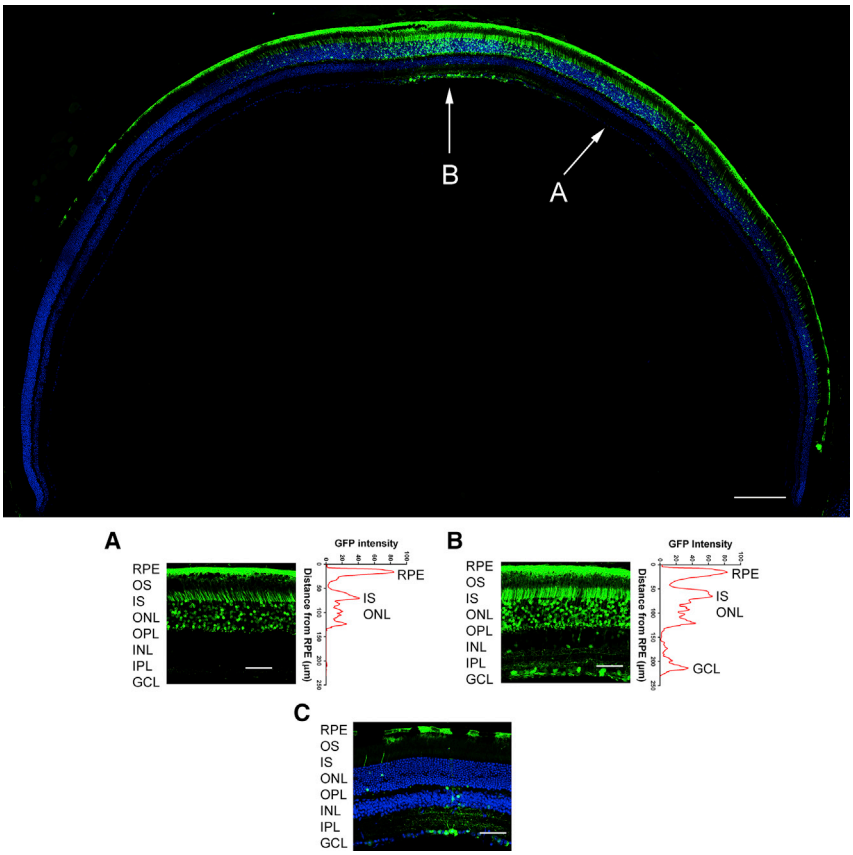

Figure 3. AAV8-GFP Vectors Penetrate All the Retinal Layers from the Vitreous with ECVM Application

WT mouse eyes were treated with ECVM (continuous direct current, 10 μA/20 min) immediately after intravitreal delivery of AAV8-CMV-EGFP (5×10^8 vg/eye) and collected 5 weeks after injection. Vector-injected WT eyes without ECVM application served as controls. The representative large image of the unimmunostained retina in cross-section of vector-injected ECVM-treated eyes illustrates distribution of transduced cells in the retina, showing original GFP fluorescence throughout the retinal layers. This image shows the GFP signal without using an anti-GFP antibody. In this example, about three-quarters of the entire length of the RPE and ONL regions was transduced to some degree by the AAV8-GFP vector. The large image of control section injected with AAV8-EGFP vector but without current is shown in the Supplement Information (Figure S3). Scale bar: 200 μm. (A and B) Higher magnification images show fluorescence profiles across the retinal thickness. GFP signals were observed in RPE and ONL (photoreceptors) (A) or in nearly all retinal layers (B). Scale bar: 50 μm. (C) Higher magnification image of control section injected with AAV8-EGFP vector but without current. GCL, ganglion cell layer; INL, inner nuclear layer; IPL, inner plexiform layer; IS, inner segments; ONL, outer nuclear layer; OPL, outer plexiform layer; OS, outer segments; RPE, retinal pigment epithelium.

layers of ECVM-treated eyes (Figure 3). Most retinal sections showed greatest GFP fluorescence by deeper retinal cells, in the RPE and photoreceptors (Figure 3A). Some sections showed transduction of ganglion cells in addition (Figure 3B). This was confirmed by the retinal distribution profile of GFP intensity. In contrast, control sections from eyes that did not receive trans-ocular current showed much less GFP expression and less extent of GFP signals across retina (Figure 3C; Figure S3).

DISCUSSION

This study demonstrates a safe, efficient, and non-invasive method to enhance gene transduction efficacy in the retina following intravitreal administration of AAV vectors. We found that applying an electric micro-current across the eye *in vivo*, ECVM, with intravitreal vector dosing augments vector penetration of the internal limiting membrane (ILM) at the retinal surface and increases transduction of cells in the outer retina. The continuous 10 μA DC for 20 min was safe for the adult mouse eye. This approach has the potential for human application, because trans-ocular current has been used safely in other contexts.[39,40,42]

Intravitreal injection is favored over the subretinal vector administration because it is less invasive for vector delivery. Human clinical intravitreal injection of drugs is now quite common in using anti-VEGF compounds to treat neovascular complications of age-related macular degeneration[43] and diabetic retinopathy.[44] Currently, however, AAV delivery by intravitreal injection has limited capacity to transduce retinal cells, especially the RPE and photoreceptors. This proof-of-concept study provides a rationale for a novel and promising delivery approach that combines ECVM with intravitreal injection of AAV vectors, and it has the potential for broad transduction to enhance retinal penetration.

Vector Stability and Mobility in an Electric Field

There is limited knowledge of how an electric field affects stability and mobility of AAV vectors. High voltages are known to affect norovirus stability.[31] Noroviruses cause foodborne illnesses and are similar to AAV viruses, because both have icosahedral geometries, no envelope, are 20–38 nm in diameter, and carry negative surface charge in a neutral buffer. For electro-separation to isolate noroviruses from samples *in vitro* using electric current as the driving force, effects of currents and buffers were evaluated on norovirus stability and mobility. Continuous 18 mA DC from 20 V for 30 min did not affect virus stability, and this caused movement of the virus in solution. Based on this, it is unlikely that our ECVM conditions of continuous 10 μA DC for 20 min would affect AAV stability. In addition, the mammalian vitreous has low ionic strength,[45] which should assist mobility.

Electric fields for iontophoresis enhance penetration of molecules including drugs, oligonucleotides, and plasmid DNA in the eyes, but our study is the first to use low-level electric current to facilitate

AAV-mediated gene transduction in the retina. We do not know the mechanisms involved. Intravitreal vectors must circumvent physical and biological barriers to reach the outer retina. Because the AAV virus carries a net negative charge in the vitreous (pH 7.4–7.52),[46] one mechanism to enhance mobility may be electro-repulsion.[47,48] Applying negative voltage at the cornea might enhance AAV vector diffusion toward the ILM. In our study, the fundus images showed that AAV8-mediated retinal transduction was not limited to the injection site in the ECVM group. Electro-repulsion, however, may account for only part of the effect, because iontophoresis also facilitates diffusion of noncharged molecules,[49] indicating that vector penetration by ECVM may work by mechanisms beyond charge attraction or repulsion.

AAV Retinal Transduction following Intravitreal Administration

Efficient gene delivery to retinal cells after intravitreal AAV administration likely involves multiple vector-host interactions, in the vitreous, in binding to cell surface receptors at the ILM, other extracellular barriers, and a traversing complex layering of retinal cells before reaching the target.[26,50] Dalkara et al.[26] showed that AAV2, AAV8, and AAV9 viruses accumulate at the vitreoretinal junction and attach at the ILM, but that only AAV2 efficiently transduced ganglion cells in the retina following intravitreal injection. This indicates that ILM accumulation of AAV vectors itself is not sufficient to circumvent extracellular barriers. Other studies demonstrated that modifying one or more tyrosines in the AAV8 and AAV9 capsids resulted in decreased ubiquitination and proteasome-mediated degradation,[51,52] and allowed these vectors to transduce retinal ganglion cells more efficiently after intravitreal delivery,[53] consistent with multiple barriers limiting AAV8 vector movement and transduction. Consequently, even if our ECVM method facilitates AAV movement toward the retinal ILM surface, this itself is not fully efficient for cellular intraretinal AAV transduction.

Other factors may also enhance AAV8-mediated retinal transduction following intravitreal delivery with ECVM. Reports indicate that applying electric current causes transient but reversible structural changes in the INL and outer nuclear layer (ONL), including increasing internuclear spaces,[36] which could make the retina permeable to AAV particles. Of interest, retinal electric stimulation promotes expression and release of neurotrophins from Müller glial cells,[54] including basic fibroblast growth factor (bFGF, also known as fibroblast growth factor 2).[55,56] bFGF enhances AAV-mediated gene transduction in rat brain,[57] whereas Müller glial cell alterations are implicated in improving AAV retinal transduction in the degenerating rat retina.[58] Because retinal structural changes[36] and change in gene expression[56] are transient and recover within 24 h, effects from a single period of ECVM treatment may be short-lived. Similarly, effects of electric current applied to transfer oligonucleotides or plasmid DNA to the retina,[37,38] or to protect from retinal degeneration[59] are enhanced by repeated application. We are exploring whether repeating ECVM application further improves the consistency of results. We observed sample-to-sample variation in AAV8-EGFP retinal transduction when applying ECVM current. Some of this is inevitable from manipulation of the small mouse eye, but it warrants study to optimize conditions that maximize AAV transduction and/or penetration by this ECVM method.

Many labs are developing novel AAV capsids that increase retinal transduction efficiency after intravitreal delivery. The AAV2-7m8 variant, identified by *in vivo* directed evolution, gives better transduction of photoreceptors and RPE after vitreous application,[60] and tyrosine mutant AAV also enhances retinal transduction following intravitreal injection.[53,61–65] Our approach of combining intravitreal delivery with trans-ocular ECVM potentially can further augment retinal transduction efficiency from the vitreous of these evolved vector capsids.

In summary, we explored a safe and non-invasive approach by trans-ocular electric micro-current application to enhance AAV8-mediated retinal transduction after intravitreal injection. This indicates that combination of ECVM and intravitreal injection could be safe and useful for efficient transduction of AAV vectors. With the encouraging results shown in this study, it is reasonable to test this approach in large-animal models for translational studies.

MATERIALS AND METHODS

Animals

Adult WT C57BL/6J mice 8–12 weeks old (Jackson Laboratory, Bar Harbor, ME, USA) were used in all the experiments. Mice were housed in nominally 60 lux dim white fluorescent lighting on a 12-h/12-h light and dark cycle. Experimental protocols were approved by the NIH Animal Care and Use Committee and adhered to the Association for Research in Vision and Opthalmology (ARVO) Statement for the Use of Animals in Ophthalmic and Vision Research. For all procedures, anesthesia was performed with intraperitoneal ketamine (92.6 mg/kg)/xylazine (5.6 mg/kg) solution, and pupils were dilated with topical ocular 0.5% tropicamide (Alcon Laboratories) and 0.5% phenylephrine hydrochloride (Bausch & Lomb) after topical 0.5% tetracaine was applied to the eye.

Adeno-Associated Virus Serotype 8 Vector

The adeno-associated virus serotype 8 (AAV8)-CMV-EGFP vector has a CMV promoter, a chimeric CMV/human β-globin intron, the EGFP gene, and a human β-globin polyadenylation (PolyA) site. Recombinant AAV was produced by the triple-transfection method and purified by polyethylene glycol precipitation followed by cesium chloride density-gradient fractionation, as previously described.[66] The purified AAV vectors were formulated in 10 mM Tris-HCl, 180 mM NaCl (pH 7.4), and 0.001% Pluronic F-68 (pH 7.4), and stored at −80°C. Quantification of vectors was done by real-time PCR using linearized plasmid standards.

Intravitreal Injection and Ocular ECVM Application

AAV8-CMV-EGFP vector dilutions 5×10^8 or 1×10^9 vg/eye were administered by intravitreal injection to adult WT mice. Mice were first anesthetized and pupils dilated. Animals were positioned under a dissecting microscope with the injected eye facing upward.

AAV8-EGFP 1 μL suspension was injected into the vitreous through the nasal sclera approximately 1 mm posterior to the limbus using a 35G beveled-tip needle attached to a 10-μL Nanofil syringe (World Precision Instruments, Sarasota, FL, USA). Triple-antibiotic ophthalmic ointment of neomycin, polymyxin B, and bacitracin was applied to the eye. Injected eyes then received ECVM application immediately (~5 min) after injection. Animals were kept on a warming pad at 32°C–33°C. Injected eyes without electric current application served as controls.

Due to the very small size of the mouse eye and vitreous cavity, retinal injury sometimes occurred by touching the retina with the needle tip opposite the entry site. When we observed evident retinal damage on OCT, some of these eyes showed widespread GFP expression. We excluded those eyes from our analysis. This occurred in 6 eyes of 65 eyes injected.

Trans-ocular ECVM Application

Mice were anesthetized, and a gold wire ring electrode was placed on the center of cornea with a thin layer of GONAK Hypromellose (Akorn, Lake Forest, IL, USA) or PBS to maintain corneal moisture. Care was taken to use minimal fluid on the cornea so as not to electrically short-circuit the cornea to the lid. A subdermal needle electrode was inserted subcutaneously on the forehead above the same eyelid. The two electrodes were separated by approximately 1 cm. Previous studies of trans-ocular electric current for neuroprotection used biphasic 1.5–300 μA for 30–60 min, which was safe for the rodent eye with retinal degeneration.[39] We initially tested 10 and 50 μA continuous DC for 20 min with the negative electrode on the cornea using a constant current stimulus isolator (A365; World Precision Instruments, Sarasota, FL, USA). These currents were achieved with less than 3 or 4 V applied. A 50-μA current application caused cornea scarring adjacent to the electrode ring and occasional cataract, whereas a 10-μA current caused no complications. To evaluate retinal safety, baseline electroretinogram (ERG) recordings (methods provided previously[67,68]; also see below) were made in seven mice, and 10 μA DC was applied to the cornea 1 week later for 20 min; ERG function was tested again 3 weeks after current application. Compared with baseline, retinal ERG function of rod and cone responses showed no change to amplitude or timing after 10 μA DC, and the intensity-response curves of a- and b-wave responses were unchanged. Eyes were removed 3 days later for retinal histology (methods provided previously[69]; also see below), and both morphology and ONL thickness were unaffected compared with untreated C57BL/6J mice, which served as controls. The results of retinal ERG, morphology, and ONL thickness are provided in the Supplemental Information (Figures S1 and S2). We selected the 10-μA current for further testing in mice.

GFP Expression by *In Vivo* Fundus Imaging

Four to six weeks after intravitreal AAV8-EGFP application, GFP expression was evaluated by fundus imaging *in vivo* (Spectralis fundus camera; Heidelberg Engineering, Heidelberg, Germany). Mice were anesthetized and pupils dilated. Blue fluorescence fundus images were captured with an ultra-wide-field (102 degrees) lens. The GFP-positive area of the central retina was measured using an intensity threshold method with ImageJ software (https://imagej.nih.gov/ij/). In brief, the analysis used photographs with the optic disc at the center, and an intensity threshold was applied to select GFP-positive areas from background signals. The same threshold setting was used for all analyses. The area percentage of GFP expression in the graph was calculated by dividing the area of GFP signal in the central retina by the total area of the central retina.

GFP Intensity and Distribution Determined on Retinal Immunohistochemistry

Retinal immunohistochemistry was performed as described by Song et al.[69] In brief, eyes were fixed, cryoprotected, embedded, snap-frozen in Tissue-Tek O.C.T. compound (Sakura Finetek USA, Torrance, CA, USA), and cryo-sectioned at 10 μm thickness. For the analysis of the GFP intensity, cryo-sections were blocked in blocking buffer and incubated with mouse anti-GFP (1:1,000; Cell Signaling Technology, Danvers, MA, USA) primary antibody overnight at 4°C, and then incubated with anti-mouse Alexa Fluor 488 secondary antibody (1:1,000; Invitrogen, Eugene, OR, USA). Retinal nuclei were counterstained with DAPI, and sections were mounted in Fluoro-Gel buffer (Electron Microscopy Sciences, Hatfield, PA, USA) for imaging. The images were generated and analyzed by the Nikon C2 confocal microscope (Nikon, Tokyo, Japan) with NIS-elements AR software, and further edited using Adobe Photoshop CS4, Version 11.0 (Adobe Systems, San Jose, CA, USA). The same imaging setting was used for analysis of all samples. For each eye, the retinal section with the strongest GFP signal was selected. Pixel intensity and area of GFP signals were measured along the entire length of the GFP-positive ONL using a method with ImageJ software (https://imagej.nih.gov/ij/), as previously described.[70] GFP intensity was expressed and plotted as pixel per area (mean ± SEM) for each group (N = 11 for each group). To analyze GFP distribution in retinas, we used micrographs of representative retinal sections without immunostaining showing average intensity Z projection of original GFP signals and plotted GFP intensity against distance from RPE using the Plot Profile function in ImageJ.

Histology

For retinal histologic analysis, cryosections were stained with H&E and photographed using a Nikon C2 confocal microscope with DS-Ri2 digital camera (Nikon, Tokyo, Japan). The thickness was evaluated by counting rows of nuclei across the ONL width at 200-μm intervals in the region between 200 and 1,000 μm from the optic nerve head, in the inferior and superior halves of the retinal sections. In a single retinal section, the nuclei counts at each point in the defined regions were averaged to give an overall estimate of the ONL thickness for that retina. Nuclei were counted in ECVM-treated (n = 12) and untreated (n = 4) mice. For each group, two sections per sample were counted.

Electroretinography

Full-field Ganzfeld scotopic and photopic ERGs were recorded using an Espion E2 Electrophysiology System with a ColorDome Ganzfeld

stimulus (Diagnosys, Lowell, MA, USA) after 12-h dark adaptation. Animals were anesthetized and pupils dilated. Measurements were made on seven animals before and after ECVM application. Measurements before ECVM application served as the baseline. Responses were plotted as intensity-response functions for analysis. These ERG methods and analyses have been fully described for our lab previously.[67,68]

Statistical Analysis

Quantitative data are presented as mean ± SEM. Statistical comparisons of ERG a- and b-wave amplitudes and implicit time were done across a range of stimulus intensities using two-way ANOVA and correcting for multiple comparisons using the Holm-Sidak method in GraphPad Prism 6.07 for Windows (GraphPad Software, La Jolla, CA, USA). To compare means between two groups, we first did a D'Agostino & Pearson omnibus normality test. For datasets that passed normality test, we used Student's t test. If not, we used the Mann-Whitney test.

SUPPLEMENTAL INFORMATION

Supplemental Information includes three figures and can be found with this article online at https://doi.org/10.1016/j.omtm.2018.12.006.

AUTHOR CONTRIBUTIONS

H.S., R.A.B., and P.A.S. contributed to the trial design. H.S., R.A.B., and Y.Z. performed ocular injections, collected data, and conducted immunoassays. H.S., R.A.B., H.Q., Y.Z., and P.A.S. contributed to the data analysis. H.S., R.A.B., Y.Z., and P.A.S. wrote the manuscript, drafted figures, tables, and supplementary information, and edited the manuscript. Y.Z. and Z.W. were responsible for the vector design and production of clinical material. All authors approved the final manuscript.

ACKNOWLEDGMENTS

We thank Jinbo Li and Maria Santos for technical assistance, and Brett Jeffrey (NEI, NIH) and Wei Li (NEI, NIH) for critical comments on the manuscript. The study was supported by the NIH Intramural Research Programs (Z01-DC000077, 2018) of the National Institute on Deafness and Other Communication Disorders and the National Eye Institute.

REFERENCES

1. Jacobson, S.G., Boye, S.L., Aleman, T.S., Conlon, T.J., Zeiss, C.J., Roman, A.J., Cideciyan, A.V., Schwartz, S.B., Komaromy, A.M., Doobrajh, M., et al. (2006). Safety in nonhuman primates of ocular AAV2-RPE65, a candidate treatment for blindness in Leber congenital amaurosis. Hum. Gene Ther. *17*, 845–858.

2. Maguire, A.M., Simonelli, F., Pierce, E.A., Pugh, E.N., Jr., Mingozzi, F., Bennicelli, J., Banfi, S., Marshall, K.A., Testa, F., Surace, E.M., et al. (2008). Safety and efficacy of gene transfer for Leber's congenital amaurosis. N. Engl. J. Med. *358*, 2240–2248.

3. Bainbridge, J.W., Smith, A.J., Barker, S.S., Robbie, S., Henderson, R., Balaggan, K., Viswanathan, A., Holder, G.E., Stockman, A., Tyler, N., et al. (2008). Effect of gene therapy on visual function in Leber's congenital amaurosis. N. Engl. J. Med. *358*, 2231–2239.

4. Cideciyan, A.V., Aleman, T.S., Boye, S.L., Schwartz, S.B., Kaushal, S., Roman, A.J., Pang, J.J., Sumaroka, A., Windsor, E.A., Wilson, J.M., et al. (2008). Human gene therapy for RPE65 isomerase deficiency activates the retinoid cycle of vision but with slow rod kinetics. Proc. Natl. Acad. Sci. USA *105*, 15112–15117.

5. Hauswirth, W.W., Aleman, T.S., Kaushal, S., Cideciyan, A.V., Schwartz, S.B., Wang, L., Conlon, T.J., Boye, S.L., Flotte, T.R., Byrne, B.J., and Jacobson, S.G. (2008). Treatment of leber congenital amaurosis due to RPE65 mutations by ocular subretinal injection of adeno-associated virus gene vector: short-term results of a phase I trial. Hum. Gene Ther. *19*, 979–990.

6. Maguire, A.M., High, K.A., Auricchio, A., Wright, J.F., Pierce, E.A., Testa, F., Mingozzi, F., Bennicelli, J.L., Ying, G.S., Rossi, S., et al. (2009). Age-dependent effects of RPE65 gene therapy for Leber's congenital amaurosis: a phase 1 dose-escalation trial. Lancet *374*, 1597–1605.

7. Bainbridge, J.W., Mehat, M.S., Sundaram, V., Robbie, S.J., Barker, S.E., Ripamonti, C., Georgiadis, A., Mowat, F.M., Beattie, S.G., Gardner, P.J., et al. (2015). Long-term effect of gene therapy on Leber's congenital amaurosis. N. Engl. J. Med. *372*, 1887–1897.

8. Russell, S., Bennett, J., Wellman, J.A., Chung, D.C., Yu, Z.F., Tillman, A., Wittes, J., Pappas, J., Elci, O., McCague, S., et al. (2017). Efficacy and safety of voretigene neparvovec (AAV2-hRPE65v2) in patients with RPE65-mediated inherited retinal dystrophy: a randomised, controlled, open-label, phase 3 trial. Lancet *390*, 849–860.

9. Bessant, D.A., Ali, R.R., and Bhattacharya, S.S. (2001). Molecular genetics and prospects for therapy of the inherited retinal dystrophies. Curr. Opin. Genet. Dev. *11*, 307–316.

10. Daiger, S.P.; University of Texas Health Science Center. (2018). RetNet: summaries of genes and loci causing retinal diseases. https://sph.uth.edu/retnet/sum-dis.htm.

11. Ali, R.R., Reichel, M.B., De Alwis, M., Kanuga, N., Kinnon, C., Levinsky, R.J., Hunt, D.M., Bhattacharya, S.S., and Thrasher, A.J. (1998). Adeno-associated virus gene transfer to mouse retina. Hum. Gene Ther. *9*, 81–86.

12. Auricchio, A., Kobinger, G., Anand, V., Hildinger, M., O'Connor, E., Maguire, A.M., Wilson, J.M., and Bennett, J. (2001). Exchange of surface proteins impacts on viral vector cellular specificity and transduction characteristics: the retina as a model. Hum. Mol. Genet. *10*, 3075–3081.

13. Yang, G.S., Schmidt, M., Yan, Z., Lindbloom, J.D., Harding, T.C., Donahue, B.A., Engelhardt, J.F., Kotin, R., and Davidson, B.L. (2002). Virus-mediated transduction of murine retina with adeno-associated virus: effects of viral capsid and genome size. J. Virol. *76*, 7651–7660.

14. Allocca, M., Mussolino, C., Garcia-Hoyos, M., Sanges, D., Iodice, C., Petrillo, M., Vandenberghe, L.H., Wilson, J.M., Marigo, V., Surace, E.M., and Auricchio, A. (2007). Novel adeno-associated virus serotypes efficiently transduce murine photoreceptors. J. Virol. *81*, 11372–11380.

15. Lebherz, C., Maguire, A., Tang, W., Bennett, J., and Wilson, J.M. (2008). Novel AAV serotypes for improved ocular gene transfer. J. Gene Med. *10*, 375–382.

16. Natkunarajah, M., Trittibach, P., McIntosh, J., Duran, Y., Barker, S.E., Smith, A.J., Nathwani, A.C., and Ali, R.R. (2008). Assessment of ocular transduction using single-stranded and self-complementary recombinant adeno-associated virus serotype 2/8. Gene Ther. *15*, 463–467.

17. Igarashi, T., Miyake, K., Asakawa, N., Miyake, N., Shimada, T., and Takahashi, H. (2013). Direct comparison of administration routes for AAV8-mediated ocular gene therapy. Curr. Eye Res. *38*, 569–577.

18. Planul, A., and Dalkara, D. (2017). Vectors and gene delivery to the tetina. Annu. Rev. Vis. Sci. *3*, 121–140.

19. Liang, F.Q., Anand, V., Maguire, A.M., and Bennett, J. (2001). Intraocular delivery of recombinant virus. Methods Mol. Med. *47*, 125–139.

20. Park, S.W., Kim, J.H., Park, W.J., and Kim, J.H. (2015). Limbal approach-subretinal injection of viral vectors for gene therapy in mice retinal pigment epithelium. J. Vis. Exp. *102*, e53030.

21. Nork, T.M., Murphy, C.J., Kim, C.B., Ver Hoeve, J.N., Rasmussen, C.A., Miller, P.E., Wabers, H.D., Neider, M.W., Dubielzig, R.R., McCulloh, R.J., and Christian, B.J. (2012). Functional and anatomic consequences of subretinal dosing in the cynomolgus macaque. Arch. Ophthalmol. *130*, 65–75.

22. Jacobson, S.G., Cideciyan, A.V., Ratnakaram, R., Heon, E., Schwartz, S.B., Roman, A.J., Peden, M.C., Aleman, T.S., Boye, S.L., Sumaroka, A., et al. (2012). Gene therapy

for leber congenital amaurosis caused by RPE65 mutations: safety and efficacy in 15 children and adults followed up to 3 years. Arch. Ophthalmol. *130*, 9–24.

23. Carvalho, L.S., and Vandenberghe, L.H. (2015). Promising and delivering gene therapies for vision loss. Vision Res. *111* (Pt B), 124–133.
24. Harvey, A.R., Kamphuis, W., Eggers, R., Symons, N.A., Blits, B., Niclou, S., Boer, G.J., and Verhaagen, J. (2002). Intravitreal injection of adeno-associated viral vectors results in the transduction of different types of retinal neurons in neonatal and adult rats: a comparison with lentiviral vectors. Mol. Cell. Neurosci. *21*, 141–157.
25. Hellström, M., Ruitenberg, M.J., Pollett, M.A., Ehlert, E.M., Twisk, J., Verhaagen, J., and Harvey, A.R. (2009). Cellular tropism and transduction properties of seven adeno-associated viral vector serotypes in adult retina after intravitreal injection. Gene Ther. *16*, 521–532.
26. Dalkara, D., Kolstad, K.D., Caporale, N., Visel, M., Klimczak, R.R., Schaffer, D.V., and Flannery, J.G. (2009). Inner limiting membrane barriers to AAV-mediated retinal transduction from the vitreous. Mol. Ther. *17*, 2096–2102.
27. Cehajic-Kapetanovic, J., Le Goff, M.M., Allen, A., Lucas, R.J., and Bishop, P.N. (2011). Glycosidic enzymes enhance retinal transduction following intravitreal delivery of AAV2. Mol. Vis. *17*, 1771–1783.
28. Tshilenge, K.T., Ameline, B., Weber, M., Mendes-Madeira, A., Nedellec, S., Biget, M., Provost, N., Libeau, L., Blouin, V., Deschamps, J.Y., et al. (2016). Vitrectomy before intravitreal injection of AAV2/2 vector promotes efficient transduction of retinal ganglion cells in dogs and nonhuman primates. Hum. Gene Ther. Methods *27*, 122–134.
29. Takahashi, K., Igarashi, T., Miyake, K., Kobayashi, M., Yaguchi, C., Iijima, O., Yamazaki, Y., Katakai, Y., Miyake, N., Kameya, S., et al. (2017). Improved intravitreal AAV-mediated inner retinal gene transduction after surgical internal limiting membrane peeling in cynomolgus monkeys. Mol. Ther. *25*, 296–302.
30. Carter, B.J. (2015). Adeno-associated virus and AAV vectors for gene delivery. In Gene and Cell Therapy: Therapeutic Mechanisms and Strategies, Fourth Edition, N.S. Templeton, ed. (CRC Press), p. 89.
31. Kang, W., and Cannon, J.L. (2015). A membrane-based electro-separation method (MBES) for sample clean-up and norovirus concentration. PLoS ONE *10*, e0141484.
32. Voigt, M., de Kozak, Y., Halhal, M., Courtois, Y., and Behar-Cohen, F. (2002). Down-regulation of NOSII gene expression by iontophoresis of anti-sense oligonucleotide in endotoxin-induced uveitis. Biochem. Biophys. Res. Commun. *295*, 336–341.
33. Asahara, T., Shinomiya, K., Naito, T., and Shiota, H. (2001). Induction of gene into the rabbit eye by iontophoresis: preliminary report. Jpn. J. Ophthalmol. *45*, 31–39.
34. Berdugo, M., Valamanesh, F., Andrieu, C., Klein, C., Benezra, D., Courtois, Y., and Behar-Cohen, F. (2003). Delivery of antisense oligonucleotide to the cornea by iontophoresis. Antisense Nucleic Acid Drug Dev. *13*, 107–114.
35. Davies, J.B., Ciavatta, V.T., Boatright, J.H., and Nickerson, J.M. (2003). Delivery of several forms of DNA, DNA-RNA hybrids, and dyes across human sclera by electrical fields. Mol. Vis. *9*, 569–578.
36. Andrieu-Soler, C., Doat, M., Halhal, M., Keller, N., Jonet, L., BenEzra, D., and Behar-Cohen, F. (2006). Enhanced oligonucleotide delivery to mouse retinal cells using iontophoresis. Mol. Vis. *12*, 1098–1107.
37. Andrieu-Soler, C., Halhal, M., Boatright, J.H., Padove, S.A., Nickerson, J.M., Stodulkova, E., Stewart, R.E., Ciavatta, V.T., Doat, M., Jeanny, J.C., et al. (2007). Single-stranded oligonucleotide-mediated in vivo gene repair in the rd1 retina. Mol. Vis. *13*, 692–706.
38. Souied, E.H., Reid, S.N., Piri, N.I., Lerner, L.E., Nusinowitz, S., and Farber, D.B. (2008). Non-invasive gene transfer by iontophoresis for therapy of an inherited retinal degeneration. Exp. Eye Res. *87*, 168–175.
39. Pardue, M.T., Ciavatta, V.T., and Hetling, J.R. (2014). Neuroprotective effects of low level electrical stimulation therapy on retinal degeneration. Adv. Exp. Med. Biol. *801*, 845–851.
40. Sehic, A., Guo, S., Cho, K.S., Corraya, R.M., Chen, D.F., and Utheim, T.P. (2016). Electrical stimulation as a means for improving vision. Am. J. Pathol. *186*, 2783–2797.
41. Pardue, M.T., and Allen, R.S. (2018). Neuroprotective strategies for retinal disease. Prog. Retin. Eye Res. *65*, 50–76.
42. Eljarrat-Binstock, E., and Domb, A.J. (2006). Iontophoresis: a non-invasive ocular drug delivery. J. Control. Release *110*, 479–489.
43. Wong, T.Y., Liew, G., and Mitchell, P. (2007). Clinical update: new treatments for age-related macular degeneration. Lancet *370*, 204–206.
44. Nicholson, B.P., and Schachat, A.P. (2010). A review of clinical trials of anti-VEGF agents for diabetic retinopathy. Graefes Arch. Clin. Exp. Ophthalmol. *248*, 915–930.
45. Bishop, P. (1996). The biochemical structure of mammalian vitreous. Eye (Lond.) *10*, 664–670.
46. Chirila, T.V., and Hong, Y. (2016). The vitreous humor. In Handbook of Biomaterial Properties, Second Edition, W. Murphy, J. Black, and G. Hastings, eds. (Springer), p. 127.
47. Guy, R.H., Kalia, Y.N., Delgado-Charro, M.B., Merino, V., López, A., and Marro, D. (2000). Iontophoresis: electrorepulsion and electroosmosis. J. Control. Release *64*, 129–132.
48. Li, S.K., Jeong, E.K., and Hastings, M.S. (2004). Magnetic resonance imaging study of current and ion delivery into the eye during transscleral and transcorneal iontophoresis. Invest. Ophthalmol. Vis. Sci. *45*, 1224–1231.
49. Li, S.K., Higuchi, W.I., Kochambilli, R.P., and Zhu, H. (2004). Mechanistic studies of flux variability of neutral and ionic permeants during constant current dc iontophoresis with human epidermal membrane. Int. J. Pharm. *273*, 9–22.
50. Schultz, B.R., and Chamberlain, J.S. (2008). Recombinant adeno-associated virus transduction and integration. Mol. Ther. *16*, 1189–1199.
51. Zhong, L., Zhao, W., Wu, J., Li, B., Zolotukhin, S., Govindasamy, L., Agbandje-McKenna, M., and Srivastava, A. (2007). A dual role of EGFR protein tyrosine kinase signaling in ubiquitination of AAV2 capsids and viral second-strand DNA synthesis. Mol. Ther. *15*, 1323–1330.
52. Zhong, L., Li, B., Mah, C.S., Govindasamy, L., Agbandje-McKenna, M., Cooper, M., Herzog, R.W., Zolotukhin, I., Warrington, K.H., Jr., Weigel-Van Aken, K.A., et al. (2008). Next generation of adeno-associated virus 2 vectors: point mutations in tyrosines lead to high-efficiency transduction at lower doses. Proc. Natl. Acad. Sci. USA *105*, 7827–7832.
53. Petrs-Silva, H., Dinculescu, A., Li, Q., Min, S.H., Chiodo, V., Pang, J.J., Zhong, L., Zolotukhin, S., Srivastava, A., Lewin, A.S., and Hauswirth, W.W. (2009). High-efficiency transduction of the mouse retina by tyrosine-mutant AAV serotype vectors. Mol. Ther. *17*, 463–471.
54. Zhou, W.T., Ni, Y.Q., Jin, Z.B., Zhang, M., Wu, J.H., Zhu, Y., Xu, G.Z., and Gan, D.K. (2012). Electrical stimulation ameliorates light-induced photoreceptor degeneration in vitro via suppressing the proinflammatory effect of microglia and enhancing the neurotrophic potential of Müller cells. Exp. Neurol. *238*, 192–208.
55. Ni, Y.Q., Gan, D.K., Xu, H.D., Xu, G.Z., and Da, C.D. (2009). Neuroprotective effect of transcorneal electrical stimulation on light-induced photoreceptor degeneration. Exp. Neurol. *219*, 439–452.
56. Hanif, A.M., Kim, M.K., Thomas, J.G., Ciavatta, V.T., Chrenek, M., Hetling, J.R., and Pardue, M.T. (2016). Whole-eye electrical stimulation therapy preserves visual function and structure in P23H-1 rats. Exp. Eye Res. *149*, 75–83.
57. Hadaczek, P., Mirek, H., Bringas, J., Cunningham, J., and Bankiewicz, K. (2004). Basic fibroblast growth factor enhances transduction, distribution, and axonal transport of adeno-associated virus type 2 vector in rat brain. Hum. Gene Ther. *15*, 469–479.
58. Kolstad, K.D., Dalkara, D., Guerin, K., Visel, M., Hoffmann, N., Schaffer, D.V., and Flannery, J.G. (2010). Changes in adeno-associated virus-mediated gene delivery in retinal degeneration. Hum. Gene Ther. *21*, 571–578.
59. Morimoto, T., Miyoshi, T., Sawai, H., and Fujikado, T. (2010). Optimal parameters of transcorneal electrical stimulation (TES) to be neuroprotective of axotomized RGCs in adult rats. Exp. Eye Res. *90*, 285–291.
60. Dalkara, D., Byrne, L.C., Klimczak, R.R., Visel, M., Yin, L., Merigan, W.H., Flannery, J.G., and Schaffer, D.V. (2013). In vivo-directed evolution of a new adeno-associated virus for therapeutic outer retinal gene delivery from the vitreous. Sci. Transl. Med. *5*, 189ra76.
61. Petrs-Silva, H., Dinculescu, A., Li, Q., Deng, W.T., Pang, J.J., Min, S.H., Chiodo, V., Neeley, A.W., Govindasamy, L., Bennett, A., et al. (2011). Novel properties of tyrosine-mutant AAV2 vectors in the mouse retina. Mol. Ther. *19*, 293–301.
62. Vandenberghe, L.H., and Auricchio, A. (2012). Novel adeno-associated viral vectors for retinal gene therapy. Gene Ther. *19*, 162–168.

63. Kay, C.N., Ryals, R.C., Aslanidi, G.V., Min, S.H., Ruan, Q., Sun, J., Dyka, F.M., Kasuga, D., Ayala, A.E., Van Vliet, K., et al. (2013). Targeting photoreceptors via intravitreal delivery using novel, capsid-mutated AAV vectors. PLoS ONE *8*, e62097.

64. Mowat, F.M., Gornik, K.R., Dinculescu, A., Boye, S.L., Hauswirth, W.W., Petersen-Jones, S.M., and Bartoe, J.T. (2014). Tyrosine capsid-mutant AAV vectors for gene delivery to the canine retina from a subretinal or intravitreal approach. Gene Ther. *21*, 96–105.

65. Boyd, R.F., Sledge, D.G., Boye, S.L., Boye, S.E., Hauswirth, W.W., Komáromy, A.M., Petersen-Jones, S.M., and Bartoe, J.T. (2016). Photoreceptor-targeted gene delivery using intravitreally administered AAV vectors in dogs. Gene Ther. *23*, 400.

66. Park, T.K., Wu, Z., Kjellstrom, S., Zeng, Y., Bush, R.A., Sieving, P.A., and Colosi, P. (2009). Intravitreal delivery of AAV8 retinoschisin results in cell type-specific gene expression and retinal rescue in the Rs1-KO mouse. Gene Ther. *16*, 916–926.

67. Song, H., Bush, R.A., Vijayasarathy, C., Fariss, R.N., Kjellstrom, S., and Sieving, P.A. (2014). Transgenic expression of constitutively active RAC1 disrupts mouse rod morphogenesis. Invest. Ophthalmol. Vis. Sci. *55*, 2659–2668.

68. Marangoni, D., Vijayasarathy, C., Bush, R.A., Wei, L.L., Wen, R., and Sieving, P.A. (2015). Intravitreal ciliary neurotrophic factor transiently improves cone-mediated function in a CNGB3-/- mouse model of achromatopsia. Invest. Ophthalmol. Vis. Sci. *56*, 6810–6822.

69. Song, H., Vijayasarathy, C., Zeng, Y., Marangoni, D., Bush, R.A., Wu, Z., and Sieving, P.A. (2016). NADPH oxidase contributes to photoreceptor degeneration in constitutively active RAC1 mice. Invest. Ophthalmol. Vis. Sci. *57*, 2864–2875.

70. Jensen, E.C. (2013). Quantitative analysis of histological staining and fluorescence using ImageJ. Anat. Rec. (Hoboken) *296*, 378–381.